Available online at www.sciencedirect.com
SCIENCE DIRECT
Thermochimica Acta 439 (2005) 32–43
thermochimica acta
www.elsevier.com/locate/tca

Kinetics of thermal decomposition of aluminium hydride: I-non-isothermal decomposition under vacuum and in inert atmosphere (argon)☆

I.M.K. Ismail*, T. Hawkins

ERC Inc at Air Force Research Laboratory/PRSP, Edwards Air Force Base, CA 93523-7689, USA*

Received 20 May 2005; received in revised form 11 August 2005; accepted 13 August 2005
Available online 7 October 2005

Abstract

Recently, interest in aluminium hydride (alane) as a rocket propulsion ingredient has been renewed due to improvements in its manufacturing process and an increase in thermal stability. When alane is added to solid propellant formulations, rocket performance is enhanced and the specific impulse increases. Preliminary work was performed at AFRL on the characterization and evaluation of two alane samples. Decomposition kinetics were determined from gravimetric TGA data and volumetric vacuum thermal stability (VTS) results. Chemical analysis showed the samples had 88.30% (by weight) aluminium and 9.96% hydrogen. The average density, as measured by helium pycnometery, was 1.486 g/cc. Scanning electron microscopy showed that the particles were mostly composed of sharp edged crystallographic polyhedral such as simple cubes, cubic octahedrons and hexagonal prisms.

Thermogravimetric analysis was utilized to investigate the decomposition kinetics of alane in argon atmosphere and to shed light on the mechanism of alane decomposition. Two kinetic models were successfully developed and used to propose a mechanism for the complete decomposition of alane and to predict its shelf-life during storage. Alane decomposes in two steps. The slowest (rate-determining) step is solely controlled by solid state nucleation of aluminium crystals; the fastest step is due to growth of the crystals. Thus, during decomposition, hydrogen gas is liberated and the initial polyhedral AlH_3 crystals yield a final mix of amorphous aluminium and aluminium crystals. After establishing the kinetic model, prediction calculations indicated that alane can be stored in inert atmosphere at temperatures below 10 °C for long periods of time (e.g., 15 years) without significant decomposition. After 15 years of storage, the kinetic model predicts ∼0.1% decomposition, but storage at higher temperatures (e.g. 30 °C) is not recommended.

Keywords: Aluminium hydride; Decomposition; Shelf-life prediction; Model free kinetics; Thermal stability

1. Introduction

Alane, AlH_3, is a solid rocket fuel containing (theoretically) 10.08% by weight hydrogen. It was evaluated in the early 1960s for military applications and was formulated in propellants. This process accelerated the development of cracks in the solid propellant. Rocket motor firing was successfully completed on 300-lb motors. However, the low thermal stability of the alane used at that time resulted in the generation of excessive amounts of hydrogen gas in the solid propellant during storage. By the early 1970s, most of the development work in the USA came to an end.

Recently, the interest in alane has been renewed presumably after the development of new methods of preparation and after the discovery of new stabilizers that can slow the rate of alane decomposition and thus increase its shelf-life. With the concern about alane thermal stability, extensive physical and chemical characterization of newly produced alane is needed, especially in the area of thermal stability and hydrogen generation during long term storage.

There have been a number of publications in the open literature on preparation, characterization, decomposition kinetics and vacuum thermal stability (VTS) of alane. Depending on the method and conditions of preparation (mainly reaction times and temperatures), alane can be produced in at least six differ-

☆ Approved for public release; distribution unlimited.

* Corresponding author. Tel.: +1 661 275 5057; fax: +1 661 275 5435.
E-mail address: ismail.ismail@edwards.af.mil (I.M.K. Ismail).

0040-6031/$ – see front matter © 2005 Elsevier B.V. All rights reserved.
doi:10.1016/j.tca.2005.08.029

ent crystal forms [1]. The most stable form is α-alane which has been used in the current investigation. Other forms are β-alane and γ-alane which are meta-stable phases. Brower et al. [1] reported that in the final steps of aluminium hydride synthesis, the β and γ forms were first formed; upon further heating, they were converted to α-alane. Polarizing-light microscopy showed the crystals of the α-phase were mostly hexagonal and cubical. The γ-phase appeared as bundles of fused needles in random orientation. Another phase, γ′-alane, appeared in the examination as small multiple needles growing from one center and forming fuzzy balls [1]. From VTS experiments [1], determined by the Taliani method [2], the α-phase was the most stable form; typically its crystals (50–150 μm) decomposed between 0.5 and 2.0% after 6 days at 60 °C depending on particle size.

The heat of decomposition of aluminium hydride samples was measured experimentally in nitrogen atmosphere using a modified bomb calorimeter accommodating a small suspended heating oven containing the sample [3]. At 298 K, the calculated average enthalpy of formation was -11.4 ± 0.8 kJ/mol, absolute entropy was 30.0 ± 0.4 kJ/mol °C and Gibbs energy of formation was 45.4 ± 1.0 kJ/mol. These values indicate that alane is an unstable compound with respect to its forming elements. Thus, thermodynamically, alane should naturally decompose to yield aluminium metal and hydrogen gas.

The VTS of unstabilized and stabilized aluminium hydride samples was measured at 60 °C [4]. The objectives were to develop new methods for synthesizing an "as-received" alane then develop new methods to stabilize the product. The time taken to reach 1% level of decomposition was ∼9.5 days for the original sample and ∼12.7 days for the stabilized one. It is interesting to note that for many investigators, the VTS tests were performed at 60 °C until reaching a 1% level of decomposition by weight; however, these test conditions are somewhat arbitrary. In most cases, most of the work was performed using the original "old" Taliani method [2] or a modified one. The kinetics and mechanism of the thermal decomposition of several solvated aluminium hydride compounds have been reported by Zakharov and Tskhai [5]. The volume of decomposition products was traced as a function of time at several isothermal temperatures between 50 and 100 °C. For dry alane samples (that is, after the removal of the solvents), an s-shaped type plot was obtained during the liberation of hydrogen. The kinetics of hydrogen liberation was described by a first order autocatalytic equation. The activation energy of this step was 72.2 ± 2.5 kJ/mol.

The thermal decomposition of AlH_3 and AlD_3 was investigated using NMR [6]. Samples of alane were decomposed isothermally (at 86–127 °C); and typical s-shaped plots, correlating percent decomposition (or amount of aluminium produced) versus reaction time, t, were obtained. Each s-curve was divided into three regions; the first of which corresponded to an induction period, τ_{ind}, where the rate constant $k_1 = 1/\tau_{ind}$. The value of τ_{ind} was defined as the time taken to achieve 5% decomposition (or when the fraction of original alane converted to aluminium, α, is 0.05). In the second region, an "acceleration period" [6] was noted between $\alpha = 0.1$ and 0.6; the equation governing the kinetics in this region was $\alpha^{1/3} = k_2 t$. The third region, $\alpha = 0.6$–0.9, was defined as the deceleration region, the kinetic rate was controlled by a third equation: $\ln(1-\alpha)^{-1} = k_3 t$. The activation energies for the three regions were 97, 108 and 112 kJ/mol, respectively, within an error of 20% [6]. A comparison between decomposition kinetics of AlH_3 and AlD_3 showed that the deuteride was decomposing at a slower rate than the hydride. For example, at 107 °C, the induction period for the deuteride was five times longer than that of the hydride, and the rate constant for the deuteride (presumably in the second region) was half of that for the hydride [6]. The differences were attributed to the presence of different impurities and crystal defects in each sample and also to differences in particle size. The effect of particle size of the hydride at 107 °C was studied between 50 and 150 μm; decomposition kinetics were highly dependent on particle size [6]. For example, to achieve the complete liberation of hydrogen, it took ∼350 min for the sizes >150 μm. but only ∼90 min for the 50 μm particles. The implication of this is that the thermal stability of alane can be enhanced, to a point, simply by increasing the starting particle size of alane.

Over the past decade, significant improvement was made to produce kinetic modeling software that helped investigators to better understand the kinetics and mechanism of chemical reactions [7–19]. These programs proved to be useful in many applications. Typical commercial software is available, such as "Model Free Kinetics" by METTLER or "Thermokinetics" by NETZSCH (which was used for the work cited in this article) and AKTS-TA-Software. Basically these programs perform sophisticated computation in a logical order. For example, a set of experiments can be performed on the sample at different heating rates (*non-isothermal method*). The iso-conversion (i.e., at constant values of α) method can normally be used to start the analysis; it yields information on how the activation energy of the entire process (or its individual steps) and the pre-exponential factor(s) could be changing as the reaction progresses; that is, from $\alpha = 0$ to 1.00. With these results taken into consideration, the programs determine numerically the best kinetic model that fits the data mathematically. The thermokinetics program has several mathematical models that prescribe chemical reactions and solid state transformations. The models include *n*th order reactions, Avrami–Erofeev solid state transformation [20] and autocatalytic reactions. A single one-step model or a combination of models (more than one-step reaction) can be chosen for performing the analysis. These software programs have been used in the recent literature to investigate the thermal decomposition of many energetic materials including HMX [10–12], ammonium perchlorate [13], ammonium nitrate [14] and ammonium dinitramide [15–16]. The programs were also used to study dimerization of cyclopentadiene [17], to predict the thermal response of hazardous materials during storage [18] and the thermal aging of rocket motor propellants [19]. This type of analysis yields a wealth of information on decomposition kinetics and mechanisms of these ingredients and propellants. To our knowledge, a similar investigation or study of alane decomposition kinetics has not been reported in the open literature.

The first objective of the present work was to develop kinetic equations (or a model) that could accurately describe

the decomposition process of alane in an inert atmosphere. The second objective was to use the model and propose a mechanism for alane decomposition. The third objective was to use the model and predict the effective storage life of alane when stored at ambient conditions.

2. Experimental

2.1. Materials

The as-received α-alane samples used in the present investigation had been synthesized and stabilized using undisclosed technology likely similar to that described by Petrie et al. [4]. The samples had the following typical elemental analysis: average weight percentage of aluminium was 88.26%, of hydrogen 9.96% and of carbon 0.44%. The balance, obtained by difference, 1.54% was assigned to oxygen. The traces of carbon found by analysis, combined with a portion of the oxygen content, are probably due to contaminated residual solvent(s) used in the process (diethyl ether). Removal of the trapped final traces of solvent is difficult to achieve experimentally [4].

2.2. Vacuum thermal stability

A new twin-chamber VTS apparatus (Fig. 1) was constructed to investigate the thermal stability of alane. Each chamber had the following major components: a Pyrex tube containing the sample which was contained inside a stainless steel tube. The tube was connected to a pressure transducer and a fine metering valve. Two type-K thermocouples were attached on the outer skin of the reactor. The entire system (A or B) was placed inside an oven regulated at a chosen temperature (normally 60 °C). The samples were evacuated at room temperature for 24 h using a combination of a roughing pump and an oil diffusion pump attached to a cryogenic liquid nitrogen trap. This system was able to pump the samples down to better than 10^{-7} Torr. The metering valve was closed, and the entire system (reactor and all other accessories) was suspended inside the oven. The electrical wires for the components were passed through a hole at the top of the oven and were connected to two data acquisition modules and a power supply. The modules were connected to feed into the serial port of a laptop computer. The experimental data were saved every 2 min; including one pressure reading and two temperature readings as a function of time. A run was typically continued until the sample reached the desired level of decomposition (∼1% weight loss). These analyses often took 5–12 days.

2.3. Thermal analysis (DSC and TGA experiments)

A Mettler TGA unit (model SDTA-851e) was used with Mettler proprietary software STAR^e version 8. Ultra-high-purity argon (UHP certified purity: 99.9999% Ar) was passed through the samples at a flow rate of 60 cc/min. For the present work, special sample containers were fabricated of quartz; the assumption was made that the regular alumina sample containers used with TGA could affect the results. Because of the differences in thermal properties of quartz and those of the other materials, the calibration coefficients of TGA were determined using the quartz containers, as per the Mettler guidelines.

Before starting a test, a sample was flushed with the selected gas for 20 min to eliminate residual air present in the system. The sample was then heated at a projected constant heating rate, between 1 and 20 °C/min from room temperature to 350 °C. After terminating a run, the density of residue was determined using a Micromeritics helium micro-Accu-Pycnometer

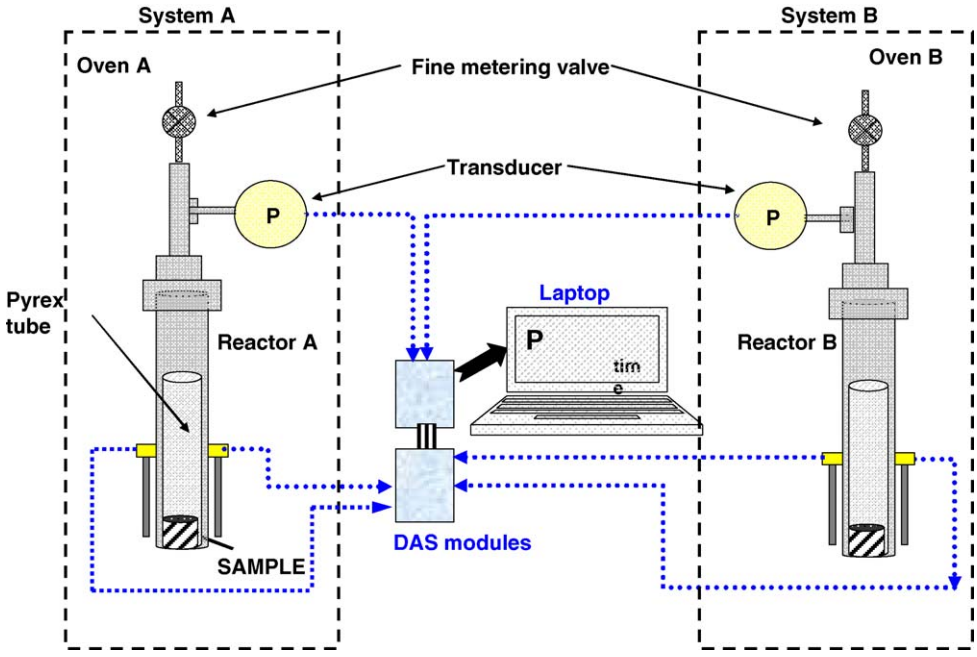

Fig. 1. Vacuum thermal stability dual system.

(cell volume: 0.25 cc and expansion volume: 0.73 cc). The surface morphology of residues was examined using SEM techniques.

The surface area and porosity development of one alane sample was studied in the following manner, using an automated surface area apparatus, Digisorb 2600, manufactured by Micromeritics Instrument Corporation. Successive runs were performed on one sample (starting weight = 0.85 g) while alternating between a pre-evacuation step at 60 °C for a given period of time, and actual measurements of surface area using krypton adsorption at −196 °C. The sample was always kept under vacuum, in He or in Kr, without ever being exposed to ambient air for the entire set of tests. This practice insured that the generated aluminium did not oxidize during the measurements. Details of this test are given next.

2.4. Calculations

Specific surface area, SA (m^2/g), was calculated from Kr adsorption isotherms obtained at liquid nitrogen temperature using the BET equation. The cross-sectional area of a Kr atom adsorbed at the surface was taken as 0.210 nm^2/Kr atom [21].

For the TGA results, the data of alane decomposition were evaluated using NETZSCH-Thermokinetics software supplied by NETZSCH-Gerätebau GmbH in Germany.

3. Results and discussion

3.1. Characterization of as-received alane

Two selected alane samples were sent to Galbraith Labs for elemental analysis (Al, H, and C assays). The results are summarized in Table 1 for the dried samples. Pure alane has a stoichiometric composition corresponding to 89.92% Al and 10.08% H. It is noted in the table that the two samples are short in Al and H because they contain other species such as C and possibly oxygen. The stoichiometric Al/H ratio is 8.921 for pure alane; the average experimental ratio was 8.86. The samples have excess (organic) H that could not be accounted for. The total percentage of Al plus H plus C did not add up to 100%; the balance can be assigned to other species; mostly oxygen. It was in the range of 1.42–1.21%.

Table 1
Chemical analysis and properties of alane

Chemical analysis	Sample 1	Sample 2
Al (%)	88.26	88.34
H (%)	9.95	9.97
C (%)	0.37	0.48
Total	98.58	98.79
Al/H ratio	8.87	8.86
Density (g/cc)	1.486	–
Surface area (m^2/g)	0.215	–

3.2. Surface area, morphology and particle size

The surface area of as-received alane, determined by krypton adsorption, was 0.215 m^2/g. This value is small and suggests that alane particles are non-porous or, at least, have an insignificant level of porosity. Fig. 2 shows the SEM photos of the two alane samples at two magnifications. These particles are not spherical, as has been noted in previous published work on alane. Instead, the particles are mostly cubes with fewer pentagonal and hexagonal crystal shapes. Occasionally, cracks and pits are noted on the surface but these are not deep. The SEM size of the particles ranges between 3 and 20 μm.

Assuming that all particles are cubical, the average size of particles, and the average equivalent length of their sides, L (in μm), can be estimated using the relation: $L = 6/(\text{surface area} \times \text{density})$. The average calculated value of L is 18.8 μm, which is in reasonable agreement with SEM observations shown in Fig. 2. It is also noted in the SEM photos that most of the particles have smooth surfaces, suggesting insignificant porosity.

3.3. Vacuum thermal stability

The effect of pre-evacuation time on decomposition kinetics of alane was studied first. Several samples were pre-evacuated at room temperature for varying periods of time: 1, 2, 10 and 16 days. There was no effect of pre-evacuation time at room temperature on subsequent decomposition kinetics at 60 °C. Therefore, a reasonable 24 h pre-evacuation time was chosen for the rest of the work reported here. Following evacuation, the sample was moved to the oven then heated to and held at 60 °C for several days. The increase in reactor pressure due to hydrogen evolution, and the corresponding percent of sample weight loss were monitored with time. When the sample reached 1% weight loss, the experiment was normally terminated and gas analyses were made using a mass-spectrometer. The main product gas was H_2 containing small trace amounts of water.

Selected results on VTS of alane are shown in Fig. 3. For the four runs performed, the results were reproducible and the time taken to reach the 1% level of weight loss was in the range of 6.8–7.6 days. An average time of 7.2 ± 0.4 days can be confidently assigned to this sample.

3.4. Development of porosity during alane decomposition

Theoretically, when alane completely decomposes to yield aluminium, the density increases from 1.486 to 2.71 g/cc. These values were confirmed in the present investigation on the starting alane and on the final products, using helium pycnometry. From the published crystallography data, the crystal size and structure should also be changing from hexagonal alane (lattice parameters: $a = 0.54$ nm and $c = 1.14$ nm) [22] to face centered cube (FCC) aluminium ($a = 0.404$ nm). Between these two extremes, one would expect a combination of the two structures, with the alane crystals breaking down and the growth of aluminium crystals. To shed more light on this effect, the following series of surface area measurements and porosity evaluations were performed on alane. A fresh alane sample

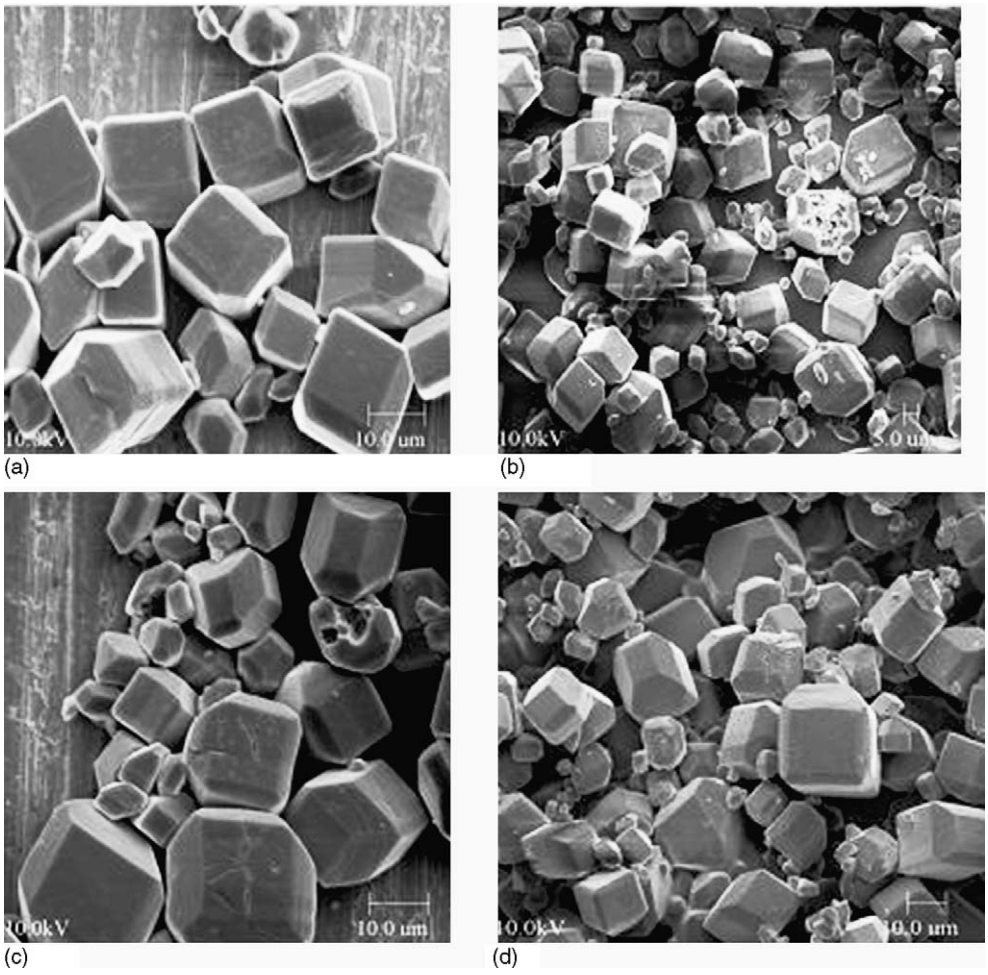

Fig. 2. SEM photos of alane at different magnifications.

(∼0.85 g) was evacuated at room temperature for 24 h; it lost 2.28%. The first Kr-surface area measurement at liquid nitrogen temperature was measured: 0.215 m^2/g. The sample was evacuated again at room temperature for an additional 24 h. There was no additional weight loss, and the surface area remained the same. The sample was again evacuated for an additional 72 h. Again, there was no weight loss or change in surface area. This means that the 2.28% loss after the first evacuation was due to evolution of moisture, trapped solvent (if any) and other volatiles.

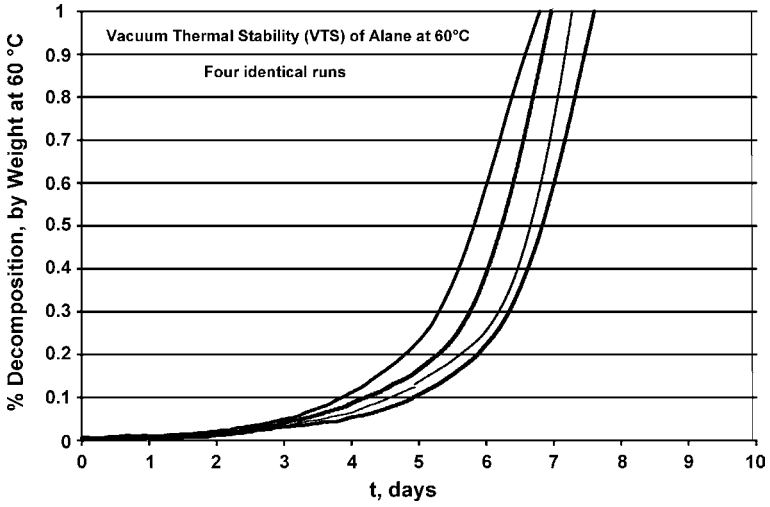

Fig. 3. Vacuum thermal stability of an alane sample at 60 °C.

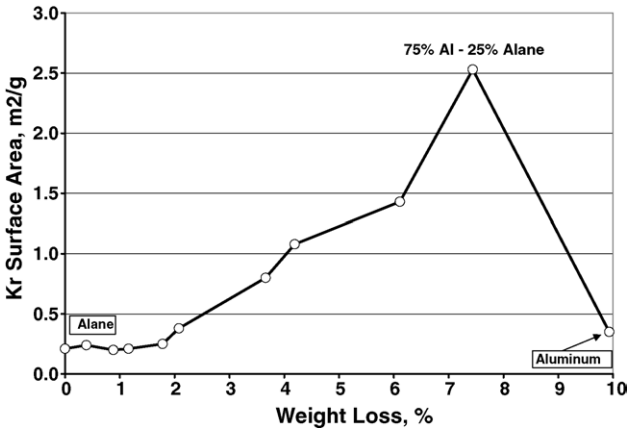

Fig. 4. Dependence of surface area of alane on extent of hydrogen evolution.

The sample was then evacuated stepwise at 60 °C for successive periods of time. After each evacuation, the sample was kept under a blanket of ultra-high-purity He to avoid possible contamination with air and to eliminate the possibility of oxidizing the fresh nascent aluminium active sites developed during hydrogen liberation. After each He fill up, the sample was weighed, and a Kr-surface area measurement was executed. These two consecutive steps were repeated several times until the final sample weight became constant; corresponding to the complete decomposition of alane. That is, the remaining weight was ∼90% of the starting weight. The results are displayed in Fig. 4. The plot has three main regions. In the first region, between 0 and 1.9% weight loss, the surface area is essentially the same. In this region there is probably loss of hydrogen atoms attached to the external surface of alane cubes plus those attached to the internal walls of open cracks, pits and crevices. The alane particles in this region are, most likely, intact; their sizes are essentially the same as the starting alane. In the second region, between ∼2 and 7.5% weight loss, the particles develop porosity as a result of the excessive hydrogen gas pressure exerted on pore walls. The walls begin cracking, the pores begin opening and the original crystal structure is opened. As more pores continue to open, the surface area keeps increasing until a maximum is reached at ∼7.5% weight loss. In the third region, the surface area drops abruptly to ∼0.35 m^2/g and remains constant at this value. This suggests that the final cubical structure of aluminium produced may only dominate after 75% of the original hydrogen evolves.

The ratio between the final specific surface area of Al and starting surface area of alane was approximately 1.63. This increase is attributed to two main reasons: a decrease in particle size after decomposition and an increase in surface roughness during decomposition. To verify this, the surfaces of several residues of partially and fully decomposed alane samples were examined using SEM. Typical representative photos are shown in Fig. 5. Plate (a) shows that the particles have developed pores and cracks after 3.1% weight loss, and that the external surface acquired slight roughness. Plate (b) shows the surface after the complete decomposition of alane. The roughness has increased drastically and there are small debris of (probably) aluminium metal covering the surface. The average particle size, for the larger particles in the completely decomposed sample, is the

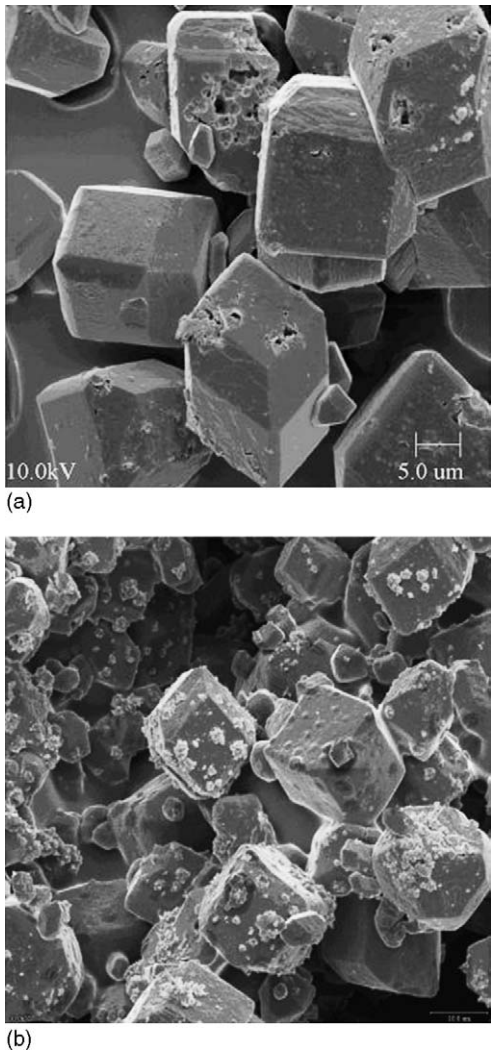

Fig. 5. SEM photos for (a) partially decomposed alane (3.1% weight loss) and (b) completely decomposed alane (∼10% weight loss).

range of 12–16 μm, compared to 18–20 μm, for the starting alane. The most interesting observation is that the original cubical and other geometrical shapes of the starting alane particles are still preserved in the final product, cubical aluminium. The experimental density of final residue after complete decomposition (plate b) was 2.69 g/cc, which is close to the theoretical value of 2.71 for pure aluminium. Thus, with this decomposition reaction, it is possible to synthesize aluminium particles in the form of cubes.

3.5. Kinetics of alane decomposition in argon

The TGA results for alane decomposition in Ar at six heating rates (0.49, 0.98, 2.0, 4.9, 9.9 and 20.2 °C/min) are shown in Fig. 6. At 20.2 °C/min, the decomposition began at 180 °C and was completed at 215 °C, and the final weight loss was 9.9%; indicating that the entire hydrogen content of alane, bonded to aluminium, had been completely removed. For the three repeated runs performed at 9.9 °C/min, the reproducibility of the data was quite satisfactory, and the average weight loss was 9.05%.

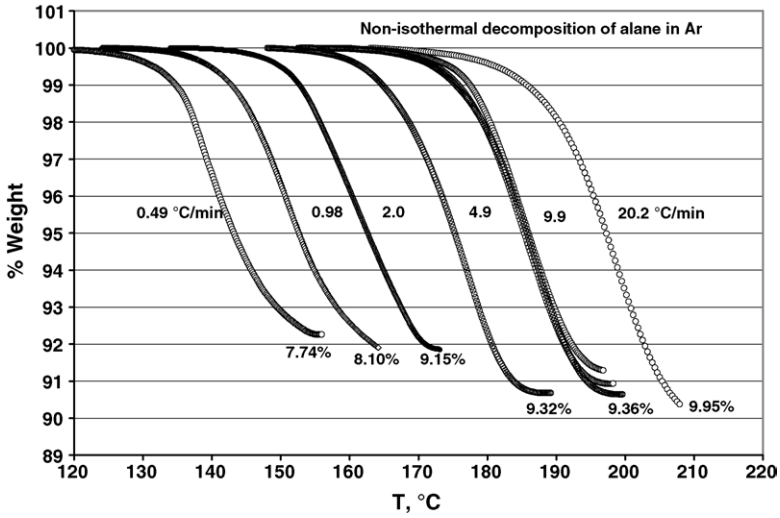

Fig. 6. Decomposition of alane in Ar (50 cc/min) at different heating rates.

The decomposition began at a lower temperature (168 °C) and was completed at 197 °C. This trend continued with the other heating rates. In all cases, the starting and final decomposition temperatures were lowered, as expected, when the heating rate decreased. The main noticeable trend is that as the heating rate decreased, the final weight loss became smaller. That is, a sample with a low heating rate retained more hydrogen than another one decomposing at a higher heating rate. It appears that when alane decomposes at a lower heating rate, the porous structure closes earlier and a portion of the hydrogen stays trapped inside the particles. Also, at a lower heating rate, decomposition occurs at lower temperatures; the diffusion of hydrogen through the particles or nucleation of aluminium sites is slow.

To perform kinetic analysis in Ar atmosphere, we pursued two independent approaches: the classical "model free kinetics" (MFK), and a more precise curve-fitting thermo-kinetics modeling (TKM) analysis. The classical MFK approach was used first to estimate the activation energy and the pre-exponential factor related to the decomposition reaction. For these classical methods, the assumption is usually made at some point of the analysis that the decomposition is a first order reaction. Based on the results of analysis with MFK, the more sophisticated TKM approach was then used with as many necessary intermediate kinetic steps and reaction orders as needed to mathematically describe the steps involved. The model showing the lowest possible standard deviation was assigned to the decomposition reaction. In the present investigation, the kinetic parameters were estimated for different types of reactions, and finally, physical models for the overall reaction were proposed.

3.5.1. Model free kinetics—iso-conversion method

The classical MFK computations include the three main well-established independent methods: the ASTM method [23], the Friedman analysis [24], and the Ozawa–Flynn–Wall analysis [25,26]. With the ASTM method, an Arrhenius plot is made between the logarithm of heating rates versus reciprocal of absolute temperatures at the points when the maximum decomposition rate occurs at each heating rate. If the plot is linear, the slope and intercept would yield the activation energy, E_a, and the pre-exponential term, A. Fig. 7 displays the results obtained with this method; the calculated values for alane decomposition are: $E_a = 97.0 \pm 3.1$ kJ/mol and $A = 2.04 \times 10^8\ s^{-1}$.

The second MFK method is the Friedman analysis [24], which is based on the iso-conversion method: at a given level of decomposition, the instantaneous decomposition rate and its corresponding temperature are calculated for each heating rate. This step is repeated at other decomposition levels until the reaction is completed. For each decomposition level (conversion), the plot between the logarithm of decomposition rate and the reciprocal of decomposition temperature would normally yield a straight line, the slope and intercept of which gives, respectively, the values of E_a and A at this particular level of decomposition. The computation is repeated for all other levels of decomposition and several lines, corresponding to several iso-conversion levels, are produced. The corresponding values of E_a and A are obtained for each level of decomposition. The results are summarized in Fig. 8. When the reaction involves more than one step, the contribution of each step to the overall kinetics will influence the observed activation energy. Thus, Fig. 8 simply suggests that alane decomposition follows, at least, two steps: the first starts and continues up to ~0.25 conversion (~2.5% weight loss for alane); and the second occurs between 0.25 and 0.85 conversion (~2.5–8.5% weight loss for alane). This finding is in line with the results of specific surface area reported above (as displayed in Fig. 4).

The third MFK method is the Ozawa–Flynn–Wall analysis [25,26] which also utilizes the iso-conversion approach. Similar to the Friedman analysis, a given conversion is first chosen. For each heating rate, the corresponding temperature is noted. A plot between the logarithm of heating rate versus reciprocal of absolute temperature is made. A linear relationship is normally obtained, and the corresponding values of E_a and A are computed for this particular conversion. The computation is repeated at other levels of conversion, and a plot is finally made between E_a and conversion (Fig. 8). This plot for alane decomposition can be interpreted in two different ways. First, one may argue that

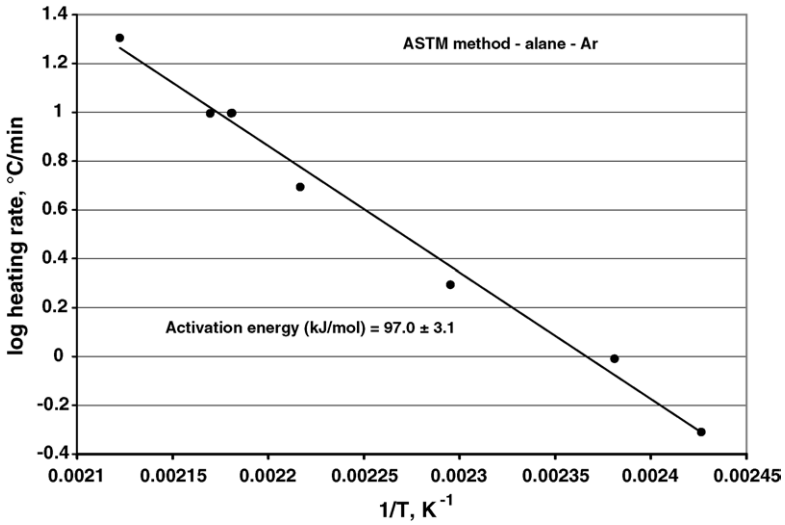

Fig. 7. Arrhenius plot for decomposition of alane in Ar using the ASTM method.

with this method, the activation energy of alane decomposition is constant through the entire reaction with an average value of 103 ± 3 kJ/mol. In this case, the decomposition of alane would follow first order kinetics. This is not the case, as will be shown shortly. Second, as was the case with the Friedman analysis, one may also argue that alane decomposition is more complicated and involves more than one step. Both scenarios will be considered next.

3.5.2. Thermokinetics modeling

Additional attempts were made to fit the original raw data to different kinetic models. The simplest model involves first order decomposition kinetics; that is: alane $\rightarrow$ aluminum + H_2. The rate of this reaction would be given by: $(d\alpha/dt) = A \times (1-\alpha) \times \exp(-E_a/RT)$, where α is the conversion fraction and R the gas constant. The analysis indicated that alane decomposition does not follow first order kinetics, as shown by the dotted (straight) lines in Fig. 9.

In the next attempts, more complicated two-step models were considered; the most promising included two-step consecutive reactions of the type: A $\rightarrow$ B $\rightarrow$ C. The two best fitting models were chosen. They are referred to here as Model-A and Model-B. Both models were statistically near perfection, with correlation coefficients better than 0.998. In both cases, Step 1 (A $\rightarrow$ B) was basically the same; it was governed by the Kolmogorov–Johnson–Mehl–Avrami (KJMA) equation (a modified Avrami equation), which describes mainly an *n*th-dimensional nucleation or growth reaction [20,27–29]. The KJMA model has been represented recently by the following equation proposed by Nakamura et al. [29]:

$$\frac{d\alpha}{dt} = n \times k(T) \times (1-\alpha) \times [-\ln(1-\alpha)]^{(n-1)/n}$$

where $k(T)$ is the rate constant, given by: $k(T) = A \times \exp(-E/RT)$. Here A is the pre-exponential factor and E is its activation energy. The Avrami exponent, n, is normally used as a tracer for the dimensionality of the reaction. Commonly accepted

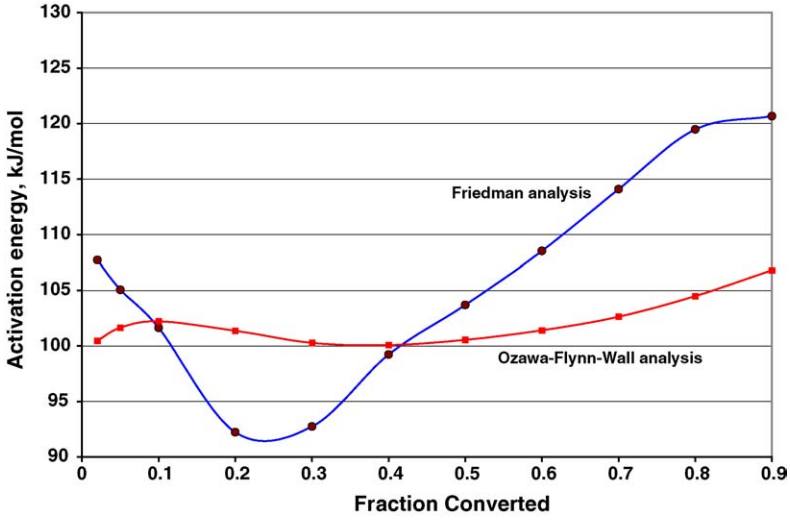

Fig. 8. Variation of activation energy with level of alane conversion to yield aluminium.

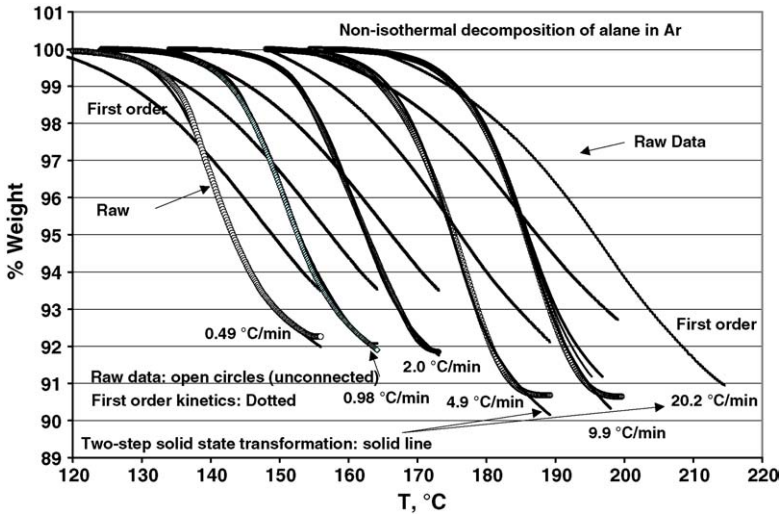

Fig. 9. Comparison between the experimental data of alane decomposition (open circles), first order decomposition kinetics model (dotted lines) and two-step reaction model (solid-line).

guidelines state that for one-dimensional growth, $n \leq 2$; for two-dimensional growth, $n = 2$–3; and for three-dimensional growth, $n = 3$–4 [29,30]. Values of the kinetic parameters obtained here for Step 1 in Model-A and Model-B are listed in Table 2.

The second step for Model-A and Model-B can be equally described statistically by two different equations. For Model A, Step 2, satisfied, once again, a second KJMA equation; the parameters of which are displayed in Table 2. They are lower than those of Step 1. However, for Model-B, the kinetics satisfied a typical chemical reaction (with nth order kinetics) of the type: $(d\alpha/dt) = A_2 \times (1-\alpha)^n \times \exp(-E_2/RT)$. In this case, the order of the reaction (power of the conversion term) was 2.52. The two models gave excellent fitting to the raw data, as indicated by the solid lines shown in Fig. 9. (Because the fitting is excellent, it may be hard to see the complete solid lines at certain regions of the plots, since the solid lines are perfectly superimposing the raw data points.) From the statistical analysis, correlation coefficients and standard deviation values, Model-A appeared slightly better than Model-B. However, Model-B could not be ruled out because its fitting to the data was also excellent.

Based on Model-A, Step 1 has a higher activation energy, pre-exponential term and Avrami exponent than Step 2 (Table 2). From the values of A, E, and n, obtained with each step, the KJMA equation was used to calculate the rate of each individual reaction, $d\alpha/dt$, at different temperatures and several values of α. Fig. 10 shows the dependence of Step 1 rates on conversion at five chosen temperatures. The rates increased with conversion, reached a maximum at $\alpha = 0.45$, and finally decreased when $\alpha > 0.45$. This trend is typical of a nucleation process. The Avrami exponent, n_1 is between 2 and 3 which suggests that the first step for alane decomposition is a two-dimensional nucleation reaction possibly taking place at the outer surface of the particles (two-dimensional nucleation).

Table 2
Calculated kinetic parameters for non-isothermal decomposition of alane in argon

	Model-A	Model-B
Step 1		
A_1 (s^{-1})	5.61×10^7	9.18×10^8
E_1 (kJ/mol)	83.8	99.0
Avrami exponent: n_1	2.23	2.43
Step 2		
A_2 (s^{-1})	4.92×10^5	3.08×10^9
E_2 (kJ/mol)	63.1	88.5
Avrami exponent: n_2	0.63	N/A
Reaction order	N/A	2.52

For Model-A, step 2 has lower values of A, E and n than Step 1. The rates for this step are much faster than in Step 1. Fig. 11 shows that the rates of Step 2 increased with temperature but decreased with increasing coverage. This step is attributed to a growth reaction; the growth of aluminium layers on the nucleation sites already developed in Step 1. The small value of n_2, which is <1, suggests that the growth reaction is a one-dimensional process, most likely, starting at the outer surface of the particles and continuing inwards towards their center.

A comparison between the rates of nucleation and growth at 100 °C is illustrated in Fig. 12. This trend was valid at all other temperatures. Since the growth rate is considerably higher than the nucleation rate, we conclude that the nucleation (surface) reaction is the rate-determining step that controls the overall decomposition of alane. This suggests that if the nucleation sites are chemically stabilized on the outer surface of the particles, the nucleation rate will be reduced and the rate of alane decomposition will be slowed.

As mentioned earlier, with Model-B, Step 1 was similar to that of Model-A; however, Step 2 was not the same. It followed a simple rate law expression of the type: $d\alpha/dt \sim (1-\alpha)^n$, where n (value = 2.52) is the overall order of the second step. One possible explanation is that the aluminium atoms, once formed after Step 1, may move over the surface and collide with each other to form metallic bonds or to enter the crystalline structure (FCC for aluminium). With this assumption, the aluminium atoms have to collide with each other at a rate of two to three times, on the aver-

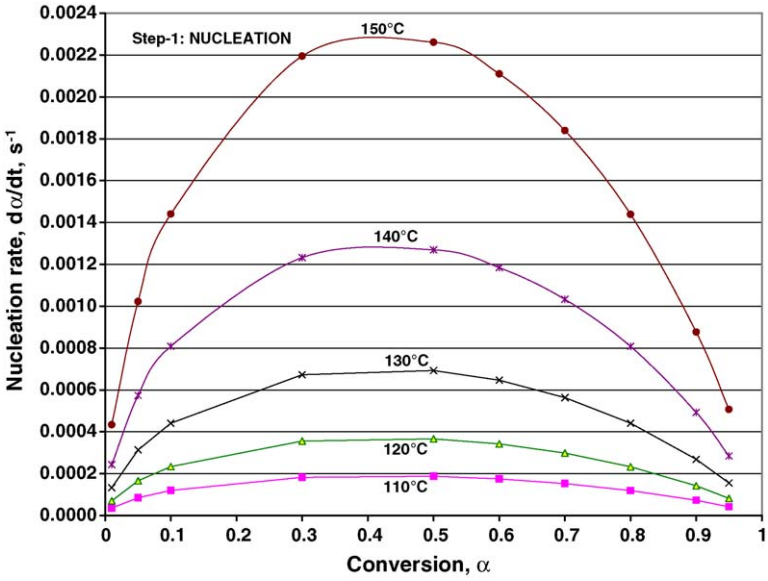

Fig. 10. Dependence of nucleation rates on conversion and temperature.

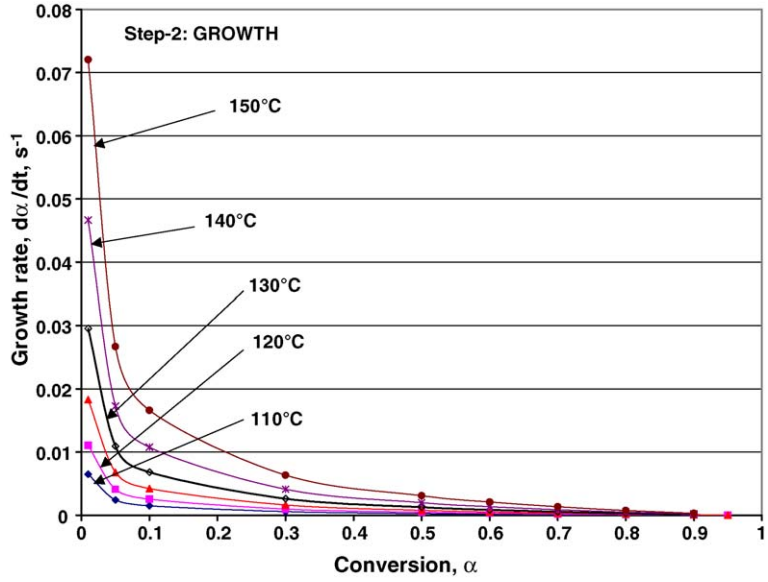

Fig. 11. Dependence of growth rates on conversion and temperature.

age, before they bond to each other. If this is the case, the number of collisions at the beginning of growth process would be high (say three or four); and it will decrease, due to the proximity of aluminium atoms, as the growth process continues. Further qualification for this mechanism is beyond the scope of this article and is left to future research.

3.6. Model prediction

With the two models developed, the prediction of alane shelf-life during storage at 5, 10, 15, 20, 25 or 30 °C was computed. The results, which are displayed in Table 3, show two significant trends. First, Model-A predicts longer shelf-life than Model-B. For example, after 3 years storage at 20 °C, while Model-A predicts 0.13% weight loss of hydrogen. Model-B predicts 1.02%

Table 3
Prediction of weight percent of hydrogen evolved during storage of alane

Years	5 °C	10 °C	15 °C	20 °C	25 °C	30 °C
(a) Model-A						
1	0.00	0.00	0.01	0.03	0.08	0.28
3	0.00	0.01	0.03	0.13	0.76	3.39
5	0.00	0.01	0.07	0.42	2.43	6.37
10	0.01	0.04	0.31	2.10	6.27	8.61
15	0.02	0.10	0.85	4.29	7.86	9.18
(b) Model-B						
1	0.00	0.01	0.03	0.10	0.42	1.74
3	0.01	0.05	0.22	1.02	3.52	5.79
5	0.03	0.14	0.68	2.76	5.27	7.22
10	0.12	0.62	2.67	5.16	7.16	9.02
15	0.29	1.47	4.19	6.24	8.28	9.77

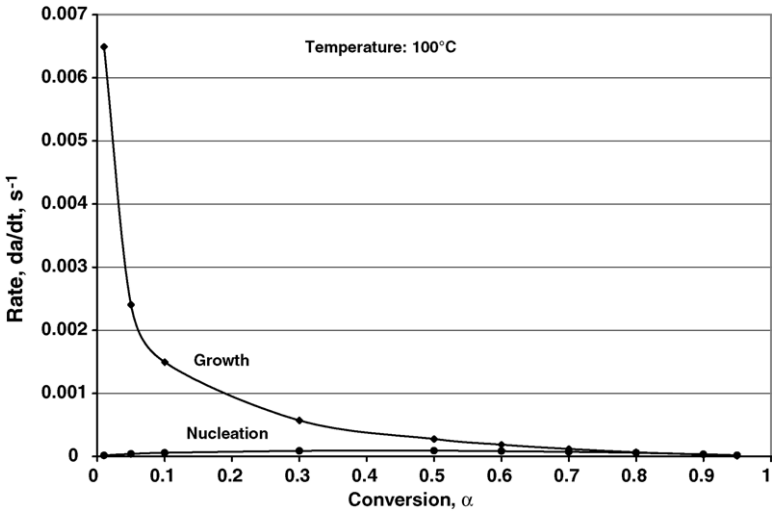

Fig. 12. Comparison between nucleation and growth rates at 100 °C.

weight loss. It is recalled from Table 1 that this sample had 9.95% elemental hydrogen content, which is smaller than the theoretical value of 10.08% by 0.13%. Since this sample has been stored in our laboratories at ambient temperature for ∼3 years, one concludes that Model-A appears more realistic for predictions than Model-B. Second, the predictions show clearly how sensitive alane decomposition is to storage temperature fluctuations. For example, if alane is stored for 10 years at 5–10 °C, the amount decomposed (as per Model-A) is insignificant; at 15 °C the sample loses 0.31%, and at 30 °C it loses most of its hydrogen (8.61%). Thus, the important critical element to extend the shelf life of alane is to store it at low temperatures, preferably in the neighborhood of 10 °C.

4. Conclusions and recommendations

1. The decomposition of alane starts with hydrogen liberation from the external surface and pre-existing pores and cracks. Porosity then increases, while the size of alane particles decreases. When the decomposition is completed, the pores are closed in the final product (aluminium).
2. The analysis of non-isothermal decomposition of alane in Ar was performed using a popular ASTM kinetic model. This approach is useful perhaps in yielding a reasonable single global value of activation energy (and pre-exponential term) that can be compared to other literature values.
3. With Freidman MFK analysis, however, alane decomposition involves two steps; this finding is supported by the results of surface area measurements.
4. Alane decomposition can be better described by solid-state transformation kinetics (nucleation and growth mechanism). Two kinetic models were developed and their fit to the experimental data was confirmed. The standard deviations for the fitting were better than 0.998. The models were used to estimate the shelf-life of alane when stored in inert atmospheres for several years.
5. Alane decomposition in Ar involves two major consecutive steps: A → B → C; representing the transformation of hexagonal alane crystals to amorphous aluminium particles (X-ray diffraction of the aluminium left after decomposition did not yield any peaks). Step 1 is due to a slow nucleation reaction; possibly with the formation of aluminium nucleation sites at the outer surface of the particles. This is the rate-determining step for alane decomposition, and the kinetics are controlled by an Avrami-type (KJMA) equation. The second step is postulated as the growth of an aluminium layer towards the center of the particles (Step 2).
6. Based on the mechanism of alane decomposition proposed here, we may suggest possible methods to further slow down the decomposition of alane. This includes coating the particles with inert materials, or formation of a protective oxide layer at the outer surface at a proper temperature. Alane oxidation at ambient temperature is insignificant, and the decomposition kinetics are not affected over the material's storage period. However, at higher temperatures, the rate of oxide formation is expected to be higher and may affect the decomposition kinetics. This is the subject of another publication in this series.
7. With Model-A developed, the projected decomposition of alane in 15 years (or less) is very small, ∼0.1%, if stored below 10 °C. Storing alane at higher temperatures is not recommended; the material may lose as much as its entire hydrogen content if stored for 15 years at 30 °C.
8. The conclusions reached here and the models developed are solely based on non-isothermal decomposition of alane in an inert atmosphere. In part II of this series (in preparation), the isothermal decomposition of alane will be addressed and the conclusions will be compared against those of non-isothermal decomposition. In part III, the effect of oxidation on alane decomposition will be addressed.

Acknowledgements

The authors want to thank Dr. Ronald Channell, Dr. Frank Roberto, Dr. Robert Corley, Dr. Keith McFall, Dr. Donald Tzeng, Mr. John Clark, Mr. Paul Jones, and Dr. George Harting for

their fruitful discussions, suggestions and support. The technical assistance of Ms Marietta Fernandez (SEM examinations) and of Ms Leslie Hudgens (density measurements) is highly appreciated.

I.M.K. Ismail is appreciative to Late Dr. J. Opfermann (at NETZSCH-Gerätebau GmbH) for his invaluable advice and the effort he made in modifying the kinetics software to meet our needs.

References

[1] F.M. Brower, N.E. Matzek, P.F. Reigler, H.W. Rinn, C.B. Roberts, D.L. Schmidt, J.A. Snovar, K. Terada, J. Am. Chem. Soc. 98 (9) (1976) 2450–2453.
[2] M. Taliani, Gazz. Chim. Ital. 51 (1921) 184.
[3] G.C. Sinke, L.C. Walker, F.L. Oetting, D.R. Stull, J. Chem. Phys. 47 (1967) 2759.
[4] M.A. Petrie, J.C. Bottaro, R.J. Schmitt, P.E. Penwell, D.C. Bomberger, United States Patent US 6,228,338 B1 (2001).
[5] V.V. Zakharov, A.N. Tskhai, Russ. J. Inorg. Chem. 37 (9) (1992) 997.
[6] V.P. Tarasov, Yu.B. Muravlve, S.I. Bakum, A.V. Novikov, Dokl. Phys. Chem. 393 (2003) 4.
[7] S.V. Vyazovkin, A.I. Lesnikovich, Thermochim. Acta 165 (1990) 273–280.
[8] S. Vyazovkin, V. Goryachko, Thermochim. Acta 194 (1992) 221–230.
[9] S. Vyazovkin, C.A. Wight, Ann. Rev. Phys. Chem. 48 (1997) 125–149.
[10] J. Opfermann, W. Haedrich, Thermochim. Acta 263 (1995) 29–50.
[11] S. Vyazovkin, C.A. Wight, Thermochim. Acta 340–341 (1999) 53–68.
[12] S. Vyazovkin, Int. Rev. Phys. Chem. 19 (2000) 45–60.
[13] S. Vyazovkin, C.A. Wight, Chem. Mater. 11 (1999) 3386–3393.
[14] S. Vyazovkin, J.S. Clawson, C.A. Wight, Chem. Mater. 13 (2001) 960–966.
[15] S. Vyazovkin, C.A. Wight, J. Phys. Chem. A 101 (1997) 8279–8284.
[16] S. Vyazovkin, C.A. Wight, J. Phys. Chem. A 101 (1997) 5653–5658.
[17] H.J. Flammersheim, J. Opfermann, Thermochim. Acta 337 (1999) 149–153.
[18] J. Opfermann, W. Haedrich, Thermochim. Acta 263 (1995) 29–50.
[19] B. Roduit, C. Borgeat, B. Berger, P. Folly, B. Alonso, J.N. Aebischer, in: Proceedings of the 31st International Pyrotechnics Seminars, 11–16 July 2004, Fort Collins, Colorado, USA.
[20] M. Avrami, J. Chem. Phys. 7 (1993) 1103–1112;
M. Avrami, J. Chem. Phys. 8 (1939) 212–224;
M. Avrami, J. Chem. Phys. 9 (1940) 177–184.
[21] I.M.K. Ismail, Langmuir 8 (1992) 360.
[22] J.W. Turley, H.W. Rinn, Inorg. Chem. 8 (1969) 18.
[23] H.E. Kissinger, J. Res. Nat. Bur. Stds. 57 (1956) 217.
[24] H.L. Friedman, J. Polym. Lett. 4 (1966) 323.
[25] T. Ozawa, Bull. Chem. Soc. Jpn. 38 (1965) 1881.
[26] J. Flynn, L.A. Wall, Polym. Lett. 4 (1966) 232.
[27] A.N. Kolmogorov, Izvestiya Acad. Nauk SSSR, Ser. Math. 1 (1937) 355.
[28] W.A. Johnson, P.A. Mehl, Trans. Am. Inst. Min. Metall. Eng. 135 (1939) 416.
[29] N. Nakamura, K. Katayama, T. Amano, J. Appl. Polym. Sci. 17 (1975) 1031.
[30] T. Pradell, D. Crespo, N. Clavaguera, M.T. Clavaguera-Mora, J. Phys.: Condens. Matter 10 (1998) 3833.